Acta Crystallographica Section B
Structural Science
ISSN 0108-7681

Studies of molecular structure parameters of 20-piperidin-2-yl-5α-pregnan-3β,20-diol and its *N*-methyl derivative: two inhibitors of $\Delta^{24(25)}$ sterol methyl transferase and $\Delta^{24(24')}$ sterol methyl reductase of *Trypanosoma cruzi*

Reinaldo Atencio,[a]* Gonzalo Visbal,[a]† Sara Pekerar,[a] Jham Papale[b] and Julio A. Urbina[b]

[a]Centro de Química, and [b]Centro de Bioquímica y Biofísica, Instituto Venezolano de Investigaciones Científicas, Apartado 21827, Caracas 1020-A, Venezuela

† Also author for correspondence; email: gvisbal@ivic.ve

Correspondence e-mail: ratencio@ivic.ve

Received 11 April 2001
Accepted 7 August 2001

Molecular structural parameters of two potential drugs against *Trypanosoma cruzi* epimastigotes, 20-piperidin-2-yl-5α-pregnan-3β,20-diol (1) and 20-*N*-methylpiperidin-2-yl-5α-pregnan-3β, 20-diol (2) were studied using a combination of a stereoselective synthetic route, spectroscopic characterization and single-crystal X-ray analysis. Both compounds were synthesized with an *R* configuration at C20. This chirality is a consequence of the stereoselectivity observed during the formation of the intermediate 20-pyridin-2-yl-5α-pregnan-3β,20*R*-diol (4). NMR data indicated that the six-membered aza ring of (2) is conformationally more restrained, in $CDCl_3$ solution, than (1). X-ray studies showed that maximum deviations among structural molecular parameters of (1) and (2) correspond to torsion angles along the C20—C22 bonds, leading to a different relative orientation of the N atom; a critical structural parameter for the binding properties of azasterols to $\Delta^{24(25)}$ sterol methyl transferase. Cremer–Pople parameters of the five-membered rings of (1) and (2) lie in the observed range for a family of tetracyclic fused ring systems retrieved from the CSD. The $\varphi 2$ parameter of (1) lies just on the mean of the family, while $\varphi 2$ of (2) deviates significantly towards the lower limit.

1. Introduction

The rational design of chemotherapeutic agents against *Trypanosoma cruzi* (the causative agent of Chagas disease) has attracted much interest due to the increasing number of humans that have contracted the chronic form of this disease and the severe limitations of currently available drugs (Docampo & Schmuñis, 1997; Mccabe, 1988; Urbina, 1997). The World Health Organization (1991) estimates that 16–18 million people are currently infected with *T. cruzi*. It has been shown that specific sterol biosynthesis inhibitors (SBI) could find useful applications as chemotherapeutic agents in the treatment of this parasitic disease (Docampo & Schmuñis, 1997; Mccabe, 1988). Currently available SBI, however, such as ketoconazole or itraconazole are not efficacious enough to eradicate *T. cruzi* from infected humans or experimental animals (Docampo & Schmuñis, 1997; Mccabe, 1988; Urbina, 1997; Brener *et al.*, 1993; Mccabe *et al.*, 1984; Wincker *et al.*, 1994; Urbina, Payares *et al.,* 1996). Other azole derivatives have recently been found to be more active as anti-*T. cruzi* agents than their currently used related compounds (Brener *et al.*, 1993; Mccabe *et al.*, 1984; Wincker *et al.*, 1994; Urbina *et al.*, 1998). More recently, the antiproliferative effects of two sterol

analogues, a cholestanol analogue with a six-membered aza-ring as a side-chain, 20-piperidin-2-yl-5α-pregnan-3β,20-diol or 22,26-azasterol (1), and 24-(*R*,*S*)25-epiminolanosterol, have been studied. Both compounds were shown to be inhibitors of $\Delta^{24(25)}$ sterol methyl transferase of epimastigotes and amastigotes of *T. cruzi* (Urbina *et ,al.*, 1995; Urbina, Vivas *et al.*, 1996).

Recent results in our laboratory have shown that alkyl substitution on the N atom of the 22,26-azasterol significantly alters both its biochemical and antiproliferative effect on *T. cruzi* epimastigotes. Sterols present in control cells (ergosterol, 24-ethyl-cholesta-5,7,22-trien-3β-ol and precursors) were almost completely replaced by zymosterol when the parasites were exposed to the minimal inhibitory concentrations of 22,26-azasterol (Urbina *et al.*, 1995). In contrast, the exposure of parasites to 20-*N*-methylpiperidin-2-yl-5α-pregnan-3β,20-diol or 22,26-*N*-methylazasterol (2) caused mostly accumulation of ergosta-5,7,22,24(24′)-tetra-en-3β-ol and ergosta-8,24(24′)-dien-en-3β-ol, suggesting an inhibitory effect on $\Delta^{24(24')}$ sterol methyl reductase, but much lower activity against $\Delta^{24(25)}$ sterol methyl transferase (Papale, 1997). These results prompted us to gain more insight on the structure–activity relationship of these potential drugs. As a first step, we report herein the study of molecular structural parameters of (1) and (2) that could be involved, at least in part, in the different biochemical activities of these sterol analogues. Structural parameters of both compounds such as absolute configuration, conformational parameters of the side-chains and their rings, especially the *D* and *E* rings (I), were evaluated by choosing a stereoselective synthetic route in combination with NMR data and X-ray studies.

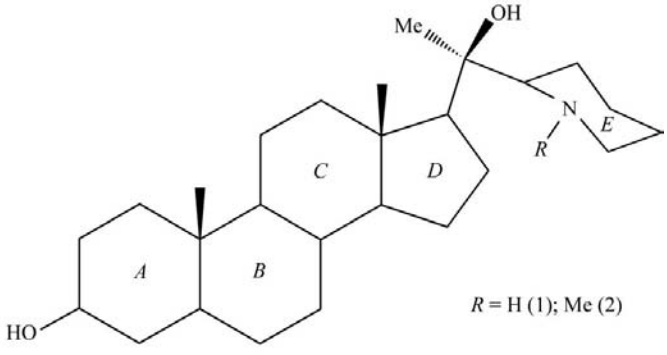

(I)

2. Experimental

2.1. General considerations

NMR spectra were obtained by using a Bruker AM-300 instrument and the spectra were recorded in $CDCl_3$. *J* values are given in Hz. All solvents were dried and distilled under N_2. FTIR spectra (in KBr disks) were obtained with a Nicolet 5DXC spectrometer.

2.2. Synthesis of 20-piperidin-2-yl-5α-pregnan-3β,20-diol (1)

To a solution of 3.30 g of (4) in 200 ml of acetic acid was added 800 mg of Adam's catalyst and the mixture was reduced with hydrogen at room temperature and atmospheric pressure. When the reaction was complete the catalyst was removed by filtration and the excess acid was partially roto-evaporated, followed by water dilution and neutralization with NH_4OH. The product was extracted with CH_3Cl, the organic phase was dried over anhydrous $MgSO_4$ and the solvent was removed by roto-evaporation. Re-crystallization was carried out with CH_3CN to yield a white solid characterized as (1) (2.92 g, 87%) m.p. 473–477 K, ν max (cm^{-1}) 3616, 3040, 2800, 1056; δ_H, 3.56 (1H, m, 3-H), 3.1 (1H, m, 26-H), 2.5 (1H, td, J = 12.5 Hz, 3H, 26-H), 1.24 (3H, s, 21-H); δ_C, 43.4 (C-13), 56.3 (C-14), 24.1 (C-15), 40.4 (C-16), 67.9 (C-17), 12.3 (C-18), 13.6 (C-19), 75 (C-20), 24.6 (C-21), 54.7 (C-22), 27.2 (C-23), 25.2 (C-24), 27 (C-25), 47.9 (C-26); *m*/*z* (EI), 403.5 (M^+, < 1%), 128 (M^+, $C_{19}H_{31}O$ 6.6%), 84 (M^+, $C_{21}H_{35}O_2$ 100%).

2.3. Synthesis of 20-*N*-methylpiperidin-2-yl-5α-pregnan-3β,20-diol (2)

Compound (6) (480 mg, 0.82 mmol) was dissolved in CH_2Cl_2 and 400 µl of concentrated HCl was added, and the mixture was left to stand for 30 min. The reaction was stopped by neutralizing with NH_4OH. The organic phase was separated, washed with H_2O, dried with $MgSO_4$ and the solvent was vacuum-evaporated. The purification of the resulting product was carried out by preparative chromatography using a mixture of ethyl acetate/toluene (1:1 v/v), (2) (83 mg, 24%); ν max (cm^{-1}) 3664, 3056, 3024, 2800, 1056, 800; δ_H 3.56 (1H, m, 3-H), 3.33 (3H, s, NCH_3), 2.82 (2H, m, 26-H), 2.45 (1H, m, 17-H), 1.25 (3H, s, 21-H), 0.81 (3H, s, 19-H), 0.77 (3H, s, 18-H); δ_C 23.4 (C-21), 55.1 (C-22), 27.2 (C-23), 25.1 (C-24), 27 (C-25), 56.3 (C-26), 37.3 (C-27); *m*/*z* (EI), 418.5 (M^+, < 1%), 98 (M^+, $C_{21}H_{35}O_2$ 100%).

2.4. Synthesis of 20-pyridin-2-yl-5α-pregnan-3β,20-diol (4)

To a solution of 27 ml of BuLi (40 mmol) in 140 ml of diethyl ether, under an argon atmosphere and at 203 K, was added a solution of 4.4 ml (40 mmol) of 2-bromopyridine in 68 ml of diethyl ether. The reaction temperature was raised to 218 K and the mixture was stirred for 30 min. After this period, the temperature was reduced to 203 K again and a solution of 5 g (14 mmol) of commercially available (3β-acetoxy-5α-pregnan-20-one, Sigma, St Louis, Missouri, USA) (3) in 208 ml of anhydrous diethyl ether was slowly added over 15 min. The reaction was stirred for 1 h at 203 K and for 2 h at 218 K. After this time, 50 ml of acetic acid was added and the reaction mixture was allowed to warm to room temperature. The aqueous phase was neutralized with Na_2CO_3 and the resulting solid was separated by extraction with ethyl acetate and filtered. The organic phase was dried over anhydrous $MgSO_4$ and the solvent was removed under vacuum. Both solids were recombined and recrystallized in CH_3CN to yield 3.48 g of (4) (3.48 g, 63%), m.p. 507–508 K; ν max (cm^{-1}) 3664, 3056, 3024, 2800, 1648, 1520; δ_H 8.44 (1H, m, 26-H), 7.64 (1H,

Table 1
Experimental details.

	(1)	(2)
Crystal data		
Chemical formula	$C_{26}H_{45}NO_2 \cdot C_2H_3N$	$C_{27}H_{47}NO_2$
Chemical formula weight	444.68	417.66
Cell setting, space group	Orthorhombic, $P2_12_12_1$	Monoclinic, $P2_1$
a, b, c (Å)	13.384 (2), 17.452 (3), 11.596 (3)	10.478 (3), 7.213 (2), 16.384 (2)
β (°)	90	99.58 (2)
V (Å^3)	2708.4 (10)	1220.9 (6)
Z	4	2
D_x (Mg m^{-3})	1.091	1.136
Radiation type	Mo $K\alpha$	Mo $K\alpha$
No. of reflections for cell parameters	21	25
θ range (°)	17 −20	16 −20
μ (mm^{-1})	0.067	0.070
Temperature (K)	293 (2)	293 (2)
Crystal form, color	Irregular block, colorless	Needle, colorless
Crystal size (mm)	0.75 × 0.60 × 0.55	0.67 × 0.30 × 0.12
Data collection		
Diffractometer	Rigaku AFC-7*S*	Rigaku AFC-7*S*
Data collection method	ω–2θ scans	ω–2θ scans
Absorption correction	Psi-scan	Psi-scan
T_{min}	0.943	0.96
T_{max}	0.971	1.00
No. of measured, independent and observed parameters	2689, 2689, 1881	4569, 4306, 3385
Criterion for observed reflections	$I > 2\sigma(I)$	$I > 2\sigma(I)$
R_{int}	0.0000	0.0220
θ_{max} (°)	25.00	25.00
Range of h, k, l	$0 \rightarrow h \rightarrow 15$ $0 \rightarrow k \rightarrow 20$ $0 \rightarrow l \rightarrow 13$	$0 \rightarrow h \rightarrow 12$ $-8 \rightarrow k \rightarrow 8$ $-19 \rightarrow l \rightarrow 19$
No. and frequency of standard reflections	3 every 150 reflections	3 every 150 reflections
Intensity decay (%)	4	0.7
Refinement		
Refinement on	F^2	F^2
$R[F^2>2\sigma(F^2)]$, $wR(F^2)$, S	0.0549, 0.1408, 1.003	0.047, 0.1157, 1.037
No. of reflections and parameters used in refinement	2468, 290	4078, 274
H-atom treatment	See text	See text
Weighting scheme	$w = 1/[\sigma^2(F_o^2) + (0.1144P)^2 + 0.0000P]$, where $P = (F_o^2 + 2F_c^2)/3$	$w = 1/[\sigma^2(F_o^2) + (0.0737P)^2 + 0.1251P]$, where $P = (F_o^2 + 2F_c^2)/3$
$(\Delta/\sigma)_{max}$	0.025	0.031
$\Delta\rho_{max}$, $\Delta\rho_{min}$ (e Å^{-3})	0.35, −0.183	0.132, −0.141
Extinction method	None	*SHELXL*93 (Sheldrick, 1993)
Extinction coefficient	–	0.0233 (39)

td, J = 7.9, 1.7 Hz, 24-H), 7.30 (1H, d, J = 7.9 Hz, 23-H), 7.12 (1H, dd, J = 5, 0.9 Hz, 25-H), 5.49 (1H, s, 20-OH), 3.56 (1H, m, 3-H), 1.55 (3H, s, 21-H); δ_C, 43.6 (C-13), 56.8 (C-14), 23.7 (C-15), 40.7 (C-16), 60.5 (C-17), 12.4 (C-18), 13.5 (C-19), 75 (C-20), 28.7 (C-21), 166.2 (C-22), 121.5 (C-23), 136.9 (C-24), 119.3 (C-25), 146.5 (C-26); *m*/*z* (EI) 397 (M^+, < 1%), 122 (M^+, $C_{19}H_{31}O$, 100%).

2.5. Synthesis of 3β,20-ditetrahydropyranyloxy-20-piperidin-2-yl-5α-pregnan (5)

To a solution of 22,26-azasterol (1) (400 mg, 1 mmol) and *p*-toluenesulfonic acid (216 mg, 1.13 mmol) in 20 ml of $CHCl_3$, 3,4-dihydro-2*H*-pyran (1 ml, 11 mmol) in 6 ml of $CHCl_3$ was added. After 4 h of stirring the mixture was extracted three times (15 ml each) with an aqueous solution of $NaHCO_3$ (10% w/v), followed by three fractions (3 × 15 ml) of H_2O. The organic phase was dried with $MgSO_4$, filtered and the solvent was roto-evaporated. The white solid obtained was re-crystallized with the mixture CH_3CN/CH_3OH (5:1 v/v) and characterized spectroscopically as (5) (570 mg, 99%), ν max (cm^{-1}) 3552, 3280, 3040, 2800, 1040, 800; δ_H 4.68 (2H, m, THP methine-H), 3.89 and 3.45 (4H, m, m, THP OCH_2), 3.55 (1H, m, 3-H), 1.26 (3H, s, 21-H); δ_C, 43.5 (C-13), 56.2 (C-14), 24.1 (C-15), 40.4 (C-16), 67.9 (C-17), 12.3 (C-18), 13.6 (C-19), 75 (C-20), 24.6 (C-21), 54.7 (C-22), 27.2 (C-23), 25.1 (C-24), 27 (C-25), 48 (C-26), 96.5 (C-27), 96.8 (C-27′), 37 (C-28), 36.1 (C-28′), 25.5 (C-29), 29.4 (C-29′), 62.9 (C31), 62.7 (C31′); *m*/*z* (EI) 572 (M^+, < 1%), 489 (M^+, C_5H_9N, < 1%), 85 (M^+, $C_{31}H_{53}O_3N$ 100%), 84 (M^+, $C_{31}H_{52}O_4$ 100%).

2.6. Synthesis of 3β,20-ditetrahydropyranyloxy-20-*N*-methylpiperidin-2-yl-5α-pregnan (6)

The preparation of this compound was carried out from the intermediate (5). To a solution of (5) (500 mg, 0.9 mmol) in 10 ml of thf an excess of NaH (10 equiv, 9 mmol) dissolved in thf was added. After 15 min of stirring 1 ml of CH_3I was added. After 4 h, the reaction was stopped by adding distilled water. The organic phase was washed with H_2O, dried with $MgSO_4$ and the solvent was roto-evaporated. Raw material of (6) (99%, 490 mg), δ_H 4.68 (2H, m, THP methine-H), 3.89 and 3.45 (4H, m, m, THP OCH_2), 3.55 (1H, m, 3-H), 2.35 (3H, s, NCH_3), 1.26 (3H, s, 21-H).

2.7. X-ray structure determinations

Crystal data and experimental details of the X-ray analysis of (1) and (2) are listed in Table 1.[1] All measurements for X-ray determinations were performed at room temperature on a Rigaku AFC-7*S* diffractometer with graphite monochromated Mo $K\alpha$ (λ = 0.71073 Å) radiation. Data were collected using

[1] Supplementary data for this paper are available from the IUCr electronic archives (Reference: AN0583). Services for accessing these data are described at the back of the journal.

the ω–2θ scan technique to a maximum 2θ value of 50°. All weak reflections [$I < 15.0\sigma(I)$] were rescanned (maximum of 1 scan) and the counts were accumulated to ensure good counting statistics. The intensities of three representative reflections were measured after every 150 reflections. No decay correction was applied. The data were corrected for Lorentz and polarization effects. A semi-empirical absorption correction (North *et al.*, 1968) based on azimuthal scans of several reflections was applied. Both structures were solved using the *SIR*92 (Altomare *et al.*, 1994) program and expanded using Fourier techniques (Sheldrick, 1993). The non-H atoms were refined anisotropically. H atoms were included in calculated positions, except for the aminic H atom in (1), which was included in its found position. They were refined riding on their heavy (C, N, or O) atoms with common or given isotropic displacement parameters based on the atom to which they are bonded, for (1) and (2), respectively. The final cycle of full-matrix least-squares refinement was based on F^2. Plots of $\Sigma w(|F_o| - |F_c|)^2$ *versus* $|F_o|$, reflection order in both data collection, $\sin\theta/\lambda$ and various classes of indices showed no unusual trends. Geometrical calculations including those of Cremer–Pople parameters (Cremer & Pople, 1975) were performed using the *PARST*96 program (Nardelli, 1995). All calculations were carried out on a Silicon Graphics R4000 computer.

2.8. Database study

Data were retrieved from the April 2001 version 5.21 of the CSD (Allen *et al.*, 1991; 233 218 entries) for all ordered crystal structures with an exact match between chemical and crystallographic connectivity with the tetracyclic ring system shown in (I). Different *R* substitution was allowed on the 3β oxygen and on the other C atoms of the *A* and *B* rings. Only entries for which atomic coordinates were given were considered and only if an *R* factor < 10% was obtained. All structures were examined individually. 37 entries containing 48 hits were retrieved and the Cremer–Pople parameters were calculated for each fragment. A polar scattergram was carried out using the *VISTA* program integrated to the CSD. Geometrical parameters such as distances, bond and torsion angles were also retrieved and they compare well with those observed for (1) and (2).

3. Results and discussion

The preparation of (1) and (2) was performed following (II), in which the protected 3β-acetoxy-5α-pregnan-20-one (3) was utilized as the starting material for the synthesis of 20-pyridin-2-yl-5α-pregnan-3β,20-diol (4) (Carey & Sundberg, 1993). Compound (3) has also been used as an intermediate for the preparation of 3β-acetoxy-21-hydroxy-5α-pregn-14-en-20-one (Simbi & van Heerden, 1997). The spectroscopic data of (4) showed that the pyridyl substituent is introduced to the 3β-acetoxy-5α-pregnan-20-one in a stereoselective form as only one ^{1}H NMR signal of 18-H (δ 0.79) was observed. This supported the presence of only one epimer, confirmed by crystallographic studies (*see below*) to be the $R_{(C\text{-}20)}$-(4) isomer. For the $S_{(C\text{-}20)}$-(4) epimer, molecular modelling and experimental results (Reetz *et al.* 1985) indicate that a downfield chemical shift of the 18-H protons may be expected because of the π-electron density effect of the pyridyl group on the C-18 methyl substituent. Therefore, the stereoselectivity observed suggests that the pyridyl group attack on the carbonyl group (C-20) was performed on the *si* face (Bartlett, 1980) of the fused-ring system, following the Felkin–Anh model (Cherest *et al.*, 1968; Anh & Eisenstein, 1977).

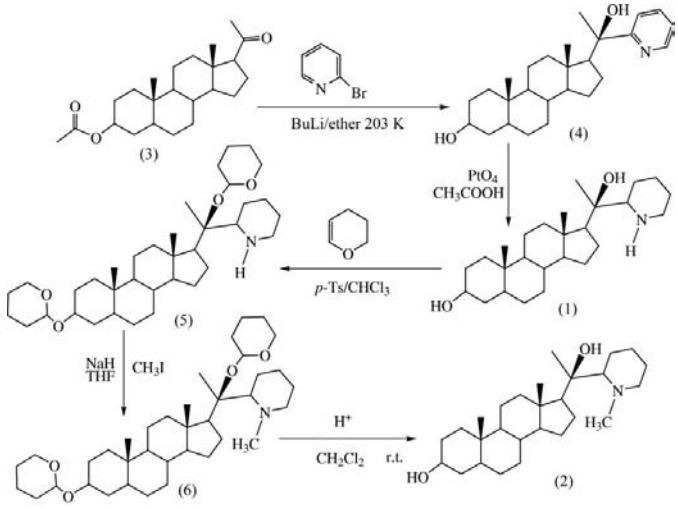

(II)

The next step was the catalytic hydrogenation of (4) using Adam's catalyst to yield 20-piperidin-2-yl-5α-pregnan-3β,20*R*-diol. The most striking characteristic of the ^{1}H NMR data for this compound was again the presence of only one signal for the C-18 protons (δ 0.76). This result confirmed the formation of the $R_{(C\text{-}20)}$-(4) isomer, see the first step of (II). For the synthesis of the 20-*N*-methylpiperidin-2-yl-5α-pregnan-3β,20*R*-diol (2), a tetrahydropyranyl group was used as a protecting agent (Parham & Anderson, 1948) for the hydroxyl substituent of (1). Methylation was, therefore, carried out in a selective form at the N atom, whereas the hydroxyl groups were conveniently regenerated upon the addition of concentrated HCl. Therefore, the synthesis allowed us to obtain both compounds with the same configuration on the C-20 atom, $R_{(C\text{-}20)}$. The significance of the C-20 stereochemistry of several sterols has recently been shown by Nes *et al.* (1997). These authors reported that cholesta-5(6),20(21),24(25)-trienol and cholesta-5,17(20)*Z*-24-trienol, in which the side chain is preferentially oriented in the left-handed conformation [$S_{(C\text{-}20)}$ configuration], failed to inhibit the activity of the $\Delta^{24(25)}$ sterol methyl transferase from *Saccharomyces cerevisiae*. In contrast, cholesta-5,20(21),24-trienol with a side chain preferentially oriented to the right [$R_{(C\text{-}20)}$ configuration] was found to be a competitive inhibitor. In similar studies Parker

& Nes (1992) generalized that sterols bind to $\Delta^{24(25)}$ sterol methyl transferase with the side chain oriented in the right-handed conformation.

For (1) and (2), NMR assignment of protons was performed using DEPT and COSY experiments. Thus, the ^{1}H NMR signals at δ 2.5 and δ 3.1 for (1), and those observed at δ 2.7 and δ 2.8 for (2), are assigned to the 26-H protons. The large difference between the 26-H chemical shifts observed for the 22,26-azasterol ($\Delta\delta$ 0.6) compared with the *N*-methyl derivative ($\Delta\delta$ 0.1) suggests that the piperidine ring of (2) has a more restrained conformational space, in $CDCl_3$ solution, than (1). Such a result appears to be a consequence of the additional steric effect caused by the methyl group on the aza-ring of (2).

The X-ray studies showed the presence of only one epimer in the crystal structures of both compounds. Views of the molecular structures of (1) and (2) are shown in Figs. 1 and 2, respectively. Considering the chiral centres of the fused tetracyclic ring system as internal references, the configurations of the C atoms in both side chains can be described as $R_{(C\text{-}20)}S_{(C\text{-}22)}$. This result confirmed the stereoselectivity observed during the preparation of the intermediate (4), as mentioned before. All C—C distances [(1): 1.506 (6)–1.556 (6) Å; (2): 1.494 (5)–1.569 (3) Å] involved in the tetracyclic system and the C—O distances [average, (1): 1.445 (5) Å; (2): 1.438 (4) Å] compare well with those previously reported from the CSD (Allen *et al.*, 1987) for similar sterol fragments. All bond and torsion angles can also be considered normal. Maximum deviations observed between (1) and (2) [mean: 10.0 (4)°] correspond to the *R*—C20—C22—N torsion angles, in which *R* represent the C17, C21 and O2 substituents. In other words, both compounds show different relative orientations of the N atom with respect to the fused ring system. Such a different orientation is probably due to the steric hindrance introduced by the N substitution. It has previously been shown that the nitrogen position and geometry are critical structural parameters for the binding properties of aza-sterol derivatives to $\Delta^{24(25)}$ sterol methyl transferase (Nes *et al.*, 1997).

A view of the hydrogen bonding observed in the crystal structure of (1) is shown in Fig. 3. The molecules aggregate using a head-to-tail connection, where the 3β-OH groups form two hydrogen bonds with the side chains of two neighbouring molecules. In the first, the 3β-OH acts as a donor in an O—H···N interaction involving the N atom of the aza-ring with H1O···N1 and O1···N1 distances of 1.914 and 2.890 (4) Å, respectively, and forming an O1—H1O···N1 angle of 159.5°. In the second hydrogen bond, the 3β-OH is the acceptor in an O—H···O intermolecular connection. In this interaction, the donor corresponds to the hydroxyl group at C-20, allowing a geometry of H2O···O1, O2···O1 and O2O—H2O···O1 of 1.908 and 2.892 (4) Å, and 175.6°, respectively.

On the other hand, in the crystal structure of (1) a CH_3CN molecule of crystallization was found (Fig. 3) directly oriented towards the N atom of the aza-ring. This result, along with the presence of the O1—H1O···N1 hydrogen bond discussed above, allowed a crystallographic differentiation between the C23 and N1 atoms. In addition, the residual electron density corresponding to the amine hydrogen was observed in the final difference map. Subsequent refinement of the position of

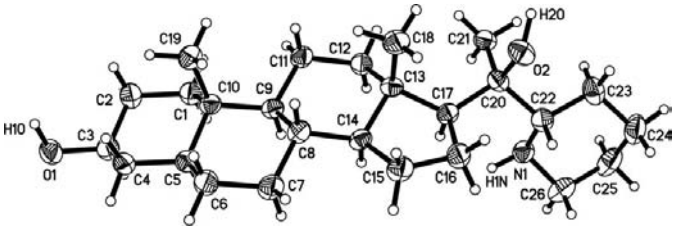

Figure 1
*ORTEP*II (Johnson, 1976) view of 20-piperidin-2-yl-5α-pregnan-3β,20-diol (1) with anisotropic displacement parameters at 35% probability.

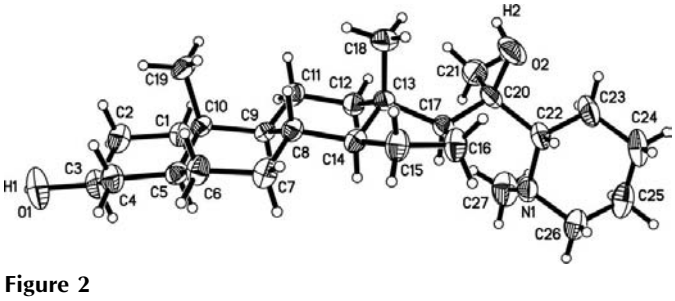

Figure 2
*ORTEP*II (Johnson, 1976) view of 20-*N*-methylpiperidin-2-yl-5α-pregnan-3β,20-diol (2) with anisotropic displacement parameters at 35% probability.

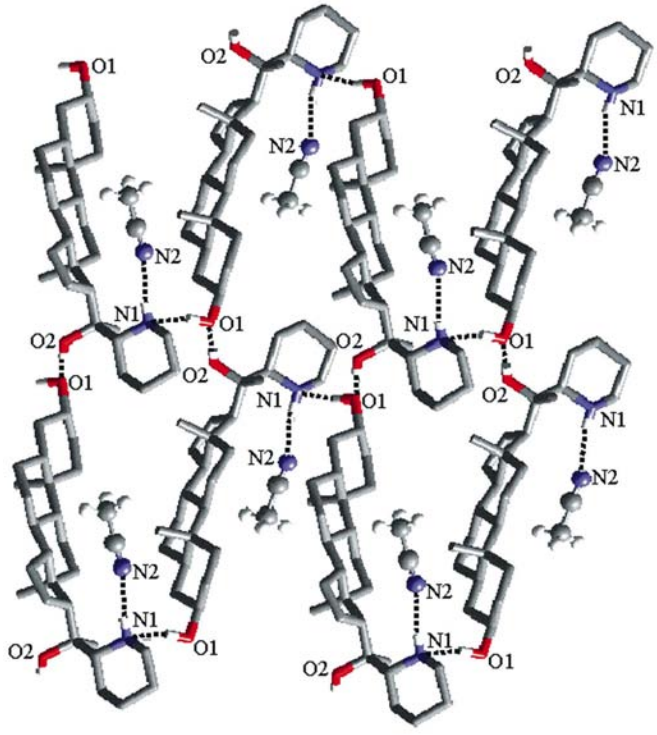

Figure 3
Hydrogen-bonding interactions observed in the crystal structure of (1). The 3β-OH participate as acceptors/donors in O—H···O(3β-OH) and O(3β-OH)—H···N(aza-ring) hydrogen bonds. In addition to this latter hydrogen bond, the amine group of the aza-ring also acts as a donor in a weak N(aza-ring)—H···N interaction involving an acetonitrile molecule.

Table 2
Cremer–Pople parameters and torsion angles of the *D* rings for (22)–(26)-azasterol (1) and *N*-methyl-22–26-azasterol (2).

Compound	Ring	Conformational parameters			
		Q_T (Å)	$\theta 2$ (°)	$\varphi 2$ (°)	$q2$ (Å)
(1)	*A* (C10,C5,C4,C3,C2,C1)	0.560 (5)	3.0 (4)	9 (8)	
	B (C10,C9,C8,C7,C6,C5)	0.557 (4)	6.4 (4)	−74 (4)	
	C (C8,C9,C11,C12,C13,C14)	0.574 (4)	3.7 (4)	−5 (5)	
	D (C14,C13,C17,C16,C15)			206.1 (5)	0.490 (4)
	E (C22,C23,C24,C25,C26,N1)	0.575 (5)	3.7 (5)	−118 (6)	
(2)	*A* (C10,C5,C4,C3,C2,C1)	0.561 (2)	2.6 (3)	−129 (6)	
	B (C10,C9,C8,C7,C6,C5)	0.565 (2)	7.7 (2)	−27 (2)	
	C (C8,C9,C11,C12,C13,C14)	0.572 (3)	2.4 (2)	53 (6)	
	D (C14,C13,C17,C16,C15)			199.0 (3)	0.472 (3)
	E (C22,C23,C24,C25,C26,N1)	0.574 (4)	2.9 (3)	−150 (6)	

D-ring torsion angles (°)	(1)	(2)
C13—C17—C16—C15	−22.0 (4)	−15.3 (3)
C14—C13—C17—C16	−42.9 (3)	−38.2 (2)
C15—C14—C13—C17	−49.2 (3)	−48.1 (2)
C16—C15—C14—C13	36.3 (4)	39.1 (2)
C17—C16—C15—C14	−8.5 (4)	−14.1 (3)

this H atom led to a non-convergent least-squares minimization. Inclusion and fixing this H-atom position allowed a weak hydrogen bond with H1N···N2 and N1···N2 distances of 2.619 and 3.447 (9) Å, respectively, and an N1—H1N···N2 angle of 147.8°. Both O1—H1O···N1 and N1—H1N···N2 hydrogen bonds could lead to a conformation of the side chain slightly different to that of the expected minimum energy. A striking feature of this hydrogen position on the N atom is that it makes the N atom a chiral centre in the solid state with a different configuration to that determined for the nitrogen centre in (2). We are currently studying reactivity and spectroscopic alternatives to gain insight into this latter observation.

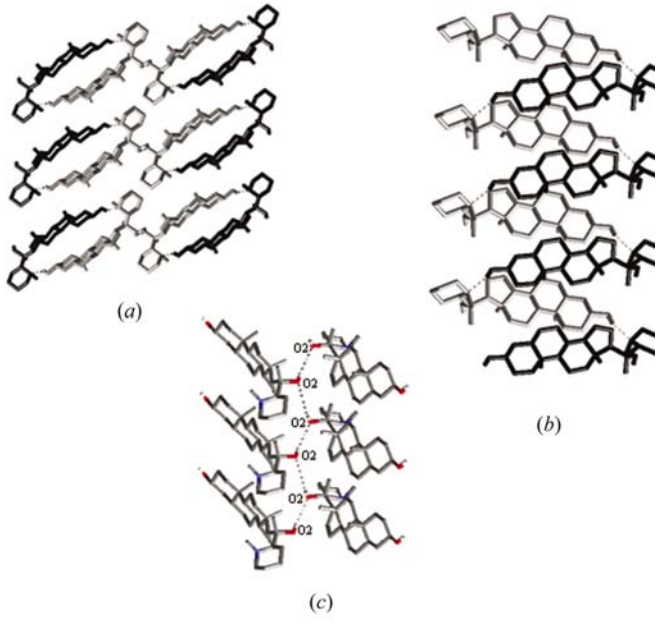

Figure 4
(*a*) View in the *b* direction of the columnar arrangement observed in the crystal structure of (2). (*b*) View of a column showing the helical arrangement. (*c*) Between two adjacent columns the hydroxyl groups at C-20 are oriented to each other to yield an O—H···O intermolecular contact with an O2—H2···O2 angle of 139.6° and an H···O2 distance of 3.149 Å resulting, probably, from a electrostatic interaction.

In the crystal structure of (2) a columnar arrangement parallel to the *b* axis can be observed (Fig. 4*a*). Two consecutive molecules in these columns adopt a head-to-tail disposition to form a helical arrangement sustained by O1—H1···N1 hydrogen bonds [H1···N1 and O1···N1 distances of 2.178 and 2.935 (3) Å, respectively, and an O1—H1···N1 angle of 153.6°; Fig. 4*b*]. In this hydrogen bond the 3β-OH participates as a donor group, whereas the N atom of the aza-ring is the corresponding acceptor. In the columnar arrangements, the hydroxyl group at C-20 is accommodated on the external side of every column. Although this hydroxyl group has a specific position in the structure no intermolecular hydrogen bonds seem to be present, probably because this compound is an acceptor-deficient molecule. However, a more detailed analysis of the intermolecular contacts reveals that two of the adjacent columns present an interdigitated assembly, allowing an O2···O2 intermolecular distance between two closer hydroxyl O atoms of 3.811 (5) Å (Fig. 4*c*). Although this distance is long enough to be considered a conventional hydrogen bond, the calculated position of the H atom on this oxygen are oriented in such a way that permit a O—H···O angle of 139.6° and a H···O distance of 3.149 Å (see Fig. 4*c*). Thus, if the electrostatic nature of a hydrogen bond is taken into account, this O—H···O intermolecular contact should not be neglected.

In Table 2 the Cremer–Pople conformational parameters (Cremer & Pople, 1975) for all rings of (1) and (2) are presented. They indicate that the six-membered rings in both compounds can be described as having the chair form ($^1C_4$; Boeyens, 1978) with very small contributions from other conformations. This table also shows, considering the puckering amplitude parameter Q_T, that atoms of all six-membered rings have a statistically equal mean deviation of the mean-plane of each ring. In both compounds, the *B* six-membered ring shows the largest distortion from the $^1C_4$ conformation (largest 2θ parameter). The five-membered ring of (1) defines a $\varphi 2$ parameter [206.1 (5)°], resulting from a linear combination, with similar contribution, of two conformations [$^2T_1(\varphi 2 = 198°) + {}^2E(\varphi 2 = 216°)$]. The same five-membered ring for (2) shows a $\varphi 2$ parameter [199.0 (3)°], very close to the pure twist $^2T_1(\varphi 2 = 198°)$ conformation. The five-membered rings present slightly different puckering amplitudes, $q2$, of 0.490 (4) and 0.472 (3) Å, for (1) and (2), respectively.

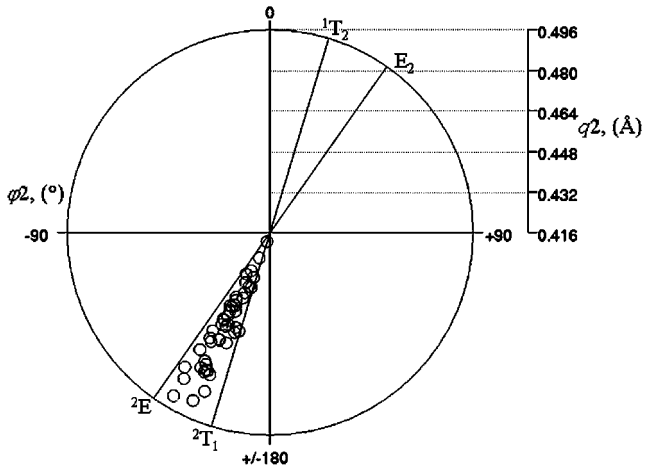

Figure 5
Polar scattergram of the Cremer–Pople parameters for the five-membered ring of 48 fused tetracyclic sterol systems retrieved from the CSD.

It is possible that the conformational differences shown by the five-membered rings in (1) and (2) could explain the different activities of such compounds as sterol biosynthesis inhibitors of *T. cruzi*. Small conformational changes on this ring could induce large conformational displacements of this class of C-20 derivative sterols. This could in turn affect the interaction of the charged nitrogen atom of the azasterol with the target enzyme's active site. We have, therefore, carried out a conformational analysis of the five-membered rings of 48 fragments retrieved from the Cambridge Structural Database (CSD; Allen *et al.*, 1991) which allows information to be obtained on the conformational preferences of this ring. Crystal structures containing at least one fused tetracyclic sterol system with the same substituents and chiralities of the *C* and *D* rings shown in (I) were considered. For each fragment, the Cremer–Pople parameters of the *D* ring were calculated and represented as a polar scattergram in Fig. 5. This figure shows how all the five-membered ring conformations lie in a close range between 197.5° ($^2T_1$ geometry) and 212.3° (close to the ^2E geometry) for the $\varphi2$ parameter, in which the average, 205.5°, represents a linear combination of the conformations $^2T_1(198°)$ and $^2E(\varphi2 = 216°)$. The puckering amplitude $q2$, on the other hand, ranges from 0.420 to 0.491 Å. The close range in $\varphi2$ was expected because this five-membered ring has two steric restrictions caused by C-17 substitution and because this ring is transfused to another six-membered cyclic system. It is appreciated that (1) has a $\varphi2$ parameter ($\varphi2 = 206.1°$) close to the mean of the family, while (2) differs significantly, probably again, due to the methyl substitution. On the other hand, the five-membered conformational space observed in all crystal structures retrieved does not show any planar conformation ($q2$ = 0 Å), but neither does it show any interconversion *pseudo*-rotational pathway ($q2$ constant and $\varphi2$ varying), suggesting that these conformational spaces should be considered of relatively high energy. This observation may be relevant to conformational behaviour in the interconversion pathway from a particular conformation into its respective enantiomeric geometry. A particular interconversion pathway, for example, from a conformation $^2T_1$ into $^1T_2$ should thus overcome high-energy geometries, suggesting a considerable degree of rigidity in this ring. It is recognized, however, that the number of geometries observed in the conformational map is somewhat limited and any interpretation from it must be carefully considered (Bürgi & Dunitz, 1994).

In summary, results presented herein are strictly related to the molecular structures of the inhibitors (1) and (2). Structural changes observed on (2) appear to be associated with the *N*-methyl substitution on the aza-ring of this compound. This methyl group raises the rigidity of the aza-ring, but at the same time seems to force the conformation along the C20—C22 bond and that of the five-membered ring, changing the relative orientation of the piperidinic N atom with respect to that observed in (1). A more dramatic structural difference between (1) and (2) was the configuration observed on the N atom of the aza-ring. Such observations may be considered in the context of the different biological activity shown by these potential drugs.

We thank the CONICIT (project S1-96001062) for partial support.

References

Allen, F. H., Davies, J. E., Galloy, J. J., Johnson, O., Kennard, O., Macrae, C. F. & Mitchell, E. M. (1991). *J. Chem. Inf. Comput. Sci.* **31**, 187–204.
Allen, F. H., Kennard, O., Watson, D. G., Brammer, L., Orpen, G. & Taylor, R. (1987). *J. Chem. Soc. Perkin Trans. 2*, pp. S1–S19.
Altomare, A., Cascarano, G., Giacovazzo, C., Guagliardi, A., Burla, M. C., Polidori, G. & Camalli, M. (1994). *J. Appl. Cryst.* **27**, 435.
Anh, N. T. & Eisenstein, O. (1977). *Nouv. J. Chim.* **1**, 61–70.
Bartlett, P. A. (1980). *Tetrahedron*, **36**, 3–97.
Boeyens, J. C. A. (1978). *J. Cryst. Mol. Struct.* **8**, 370.
Brener, Z., Cançado, J. R., Galvão, L. M., da Luz, Z. M. P., Filardi, L. D. S., Pereira, M. E. S., Santos, L. M. T. & Cançado, C. B. (1993). *Mem. Inst. Oswaldo Cruz.* **88**, 149.
Bürgi, H.-B. & Dunitz, J. D. (1994). *Structure Correlation*, Vol. 2. Weinheim: VCH.
Carey, F. A. & Sundberg, R. J. (1993). *Advanced Organic Chemistry*, Part B, 3ed ed., pp. 365–400. New York: Plenum Press.
Cherest, M., Felkin, H. & Prudent, N. (1968). *Tetrahedron Lett.* pp. 2199–2204.
Cremer, D. & Pople, J. A. (1975). *J. Am. Chem. Soc.* **97**, 1354–1358.
Docampo, R. & Schmuñis, G. A. (1997). *Parasitol. Today*, **4**, 129–130.
Johnson, C. K. (1976). *ORTEP*II. Report ORNL-5138. Oak Ridge National Laboratory, Tennessee, USA.
Mccabe, R. E. (1988). *J. Infect. Dis.* **158**, 1408–1409.
Mccabe, R. E., Remington, J. S. & Araujo, F. G. (1984). *J. Infect. Dis.* **150**, 594–601.
Nardelli, M. (1995). *J. Appl. Cryst.* **28**, 659.

Nes, W. D., Guo, D. & Zhou, W. (1997). *Arch. Biochem. Biophys.* **342**, 68–81.
North, A. C. T., Phillips, D. C. & Mathews, F. S. (1968). *Acta Cryst.* A**24**, 351–359.
Papale, J. (1997). *Magister Science Thesis.* Instituto Venezolano de Investigaciones Científicas, Venezuela.
Parham, W. E. & Anderson, E. L. (1948). *J. Am. Chem. Soc.* **70**, 4187–4189.
Parker, S. R. & Nes, W. D. (1992). *Am. Chem. Soc. Symp. Ser.* **497**, 110–145.
Reetz, M. T., Steinbach, R., Westermann, J., Peter, R. & Wenderoth, B. (1985). *Chem. Ber.* **118**, 1441–1454.
Sheldrick, G. M. (1993). *SHELXL*93. University of Göttingen, Germany.
Simbi, L. & van Heerden, F. R. (1997). *J. Chem. Soc. Perkin Trans. 1*, pp. 269–273.
Urbina, J. A. (1997). *Parasitology*, **117**, S91–S99.
Urbina, J. A., Payares, G., Contreras, L. M., Liendo, A., Sanoja, C., Medina, J., Piras, M., Piras, R., Pérez, N., Wincker, P. & Loebemberg, D. (1998). *Antimicrobiol. Agents Chemother.* **42**, 1771–1777.
Urbina, J. A., Payares, G., Molina, J., Sanoja, C., Liendo, A., Lazardi, K., Piras, M., Piras, R., Pérez, N., Wincker, P. & Ryley, J. F. (1996). *Science*, **273**, 969–971.
Urbina, J. A., Vivas, J., Lazardi, K., Molina, J., Payares, G., Piras, M. & Piras, R. (1996). *Chemotherapy*, **42**, 294–307.
Urbina, J. A., Vivas, J., Visbal, G. & Contreras, L. M. (1995). *Mol. Bio-Chem. Parasitol.* **73**, 199–210.
World Health Organization (1991). WHO Technical Report, Series No. 811.
Wincker, P., Britto, C., Borges-Pereira, J., Cardoso, M. A., Oelemann, W. & Morel, C. M. (1994). *Am. J. Trop. Med. Hyg.* **51**, 771–777.